The type of carbohydrates specifically selects microbial community structures and fermentation patterns

Lucile Chatellard, Eric Trably, Hélène Carrère

The type of carbohydrates specifically selects microbial community structures and fermentation patterns

Lucile Chatellard[a], Eric Trably[a*], Hélène Carrère[a]

[a] LBE, INRA, 102 avenue des Etangs, 11100 Narbonne, France

Abstract

The impact on dark fermentation of seven carbohydrates as model substrates of lignocellulosic fractions (glucose, cellobiose, microcrystalline cellulose, arabinose, xylose, xylan and wheat straw) was investigated. Metabolic patterns and bacterial communities were characterized at the end of batch tests inoculated with manure digestate. It was found that hydrogen production was linked to the sugar type (pentose or hexose) and the degree of polymerisation. Hexoses produced less hydrogen, with a specific selection of lactate-producing bacterial community structures. Maximal hydrogen production was five times higher on pentose-based substrates, with specific bacterial community structures producing acetate and butyrate as main metabolites. Low hydrogen amounts accumulated from complex sugars (cellulose, xylan and wheat straw). A relatively high proportion of the reads was affiliated to *Ruminococcaceae* suggesting an efficient hydrolytic activity. Knowing that the bacterial community structure is very specific to a particular substrate offers new possibilities to design more efficient H_2-producing biological systems.

Keywords

Biohydrogen; Dark fermentation; Lignocellulosic residues; Microbial consortium

1. Introduction

Energetic transition and waste management are ones of the main XXIth century challenges (UNFCCC. Conference of the Parties (COP), 2015). Among all the renewable energies nowadays available, hydrogen has a promising future. Its energy power by mass unit (122 kJ.g^{-1}) is higher than most of other energy sources and its combustion produces only water and no carbon dioxide (Saratale et al., 2008). Hydrogen gas can be produced along the bioconversion of organic matter by dark fermentation. This natural biological process is carried out by different types of microorganisms widespread in Nature and found in most of anaerobic environments, such as in lakes, guts, urban sludge or manure digestate (Wang and Wan, 2009). First hydrolytic bacteria convert the organic matter into simpler molecules and the monomeric forms can further be assimilated by fermentative hydrogen-producing bacteria. Depending on the type of bacteria and the metabolic pathway used to convert these substrates, accumulation of hydrogenated biochemical intermediates (NADH) in the cell can lead to the production of biohydrogen to recycle the reduced elements in the cell (Cai et al., 2011). More particularly, acetic and butyric acid pathways generate four and two moles of hydrogen per mole of glucose consumed, respectively (Kalia and Purohit, 2008).

In mixed cultures, other metabolic pathways that are detrimental to hydrogen production by consuming carbohydrates, such as lactic acid or alcoholic fermentation, are also observed. Furthermore, the reuse of the hydrogen produced is also possible by other groups of H_2-consuming bacteria to form other volatile fatty acids such as propionate, caproate but also acetate and methane by homoacetogenesis and methanogenesis, respectively (Saady, 2013). Although heat shock treatment has been

46 well described to get rid of the methanogenic activity, other fermentative pathways are
47 often carried out by thermo-resistant microorganisms (Wong et al., 2014).
48 Nonetheless, using mixed culture is advantageous since complex substrates such
49 as lignocellulose can also be used. The use of complex microbial consortia will increase
50 the chance to find bacteria with efficient enzymatic materials to degrade complex
51 biomass (Kleerebezem and van Loosdrecht, 2007). Lignocellulosic biomass is a
52 substrate of choice for the production of renewable energies. It is the most abundant
53 organic carbon source because it composes the major part of agricultural waste with a
54 low cost (Guo et al., 2010). But the complex structure of lignocellulosic materials can
55 impact bacterial fermentation and mechanisms are not yet well understood.
56 Lignocellulosic compounds are mainly composed of three polymers linked
57 together to form a complex matrix : lignin, cellulose and hemicelluloses (Menon and
58 Rao, 2012). Lignin is a phenolic polymer known to not be biodegradable for most of
59 bacteria. It is linked to hemicelluloses, bond to cellulose. Whereas hemicelluloses are
60 heteropolymer mainly composed of D-xylose, but also L-arabinose and D-glucose,
61 cellulose is a homopolymer of cellobiose, a dimer of glucose. Because of the polymeric
62 structure, deconstructive pre-treatment are usually applied on lignocellulosic biomass to
63 release fermentable sugars (Nissilä et al., 2014).
64 Depending on the proportion of each sugar, the polymerisation degree and other
65 biochemical parameters, fermentative pathways and performances can be both
66 impacted. This work aims to evaluate the potential of main lignocellulosic biomass
67 fractions to produce hydrogen by dark fermentation. Pure model substrates representing
68 the main fractions of lignocellulosic materials were fermented in batch reactors with the
69 same initial mixed inoculum (manure anaerobic digestate). Through the analysis of

metabolites co-produced during the process and the final bacterial community structures, the impact of the type of carbon source on microbial community function was evaluated.

2. Materials and methods

2.1. Inoculum preparation and experimental setup

The outlet of a solid-state anaerobic reactor fed with bull manure (Montrodat, France), so-called digestate, was used as initial microbial inoculum. Because undigested straw was present in the digestate, microorganisms were first extracted according to a protocole adapted from Zhang *et al* (2007). For that, 40 ml of sterile physiological water were added to 20 g of digestate in a 500 ml centrifuge tube. After dynamic hand shaking, the tube was centrifuged for 5min at 3000 g (temperature 4°C). The supernatant was recovered in a sterile bottle and the pellet was washed with 40 ml of sterile phosphate buffer at 10 mM. After shaking, the tube was again centrifuged at 3000 g during 10 min (4°C). The supernatant was recovered and added to the first one. The residual juice of the pellet was sieved at 1 mm. Heat shock pre-treatment (90°C, 30 min followed by ice cooling) was performed before inoculation to get rid of hydrogen consumption by methanogenic archaea.

Biohydrogen production potential (BHP) tests were carried out in batch tests in quadriplicates in 600 ml plasma bottle with 400 ml of working volume. The medium was composed of 12.5 ml of minimal nutrient solution (in $mg.l^{-1}$ - NH4Cl : 32000 ; K2HPO4 : 20000 ; FeCl2,4H2O : 1500 ; H3BO3,H2O : 60 ; MnSO4,H2O : 117; CoCl2,6H2O : 25 ; ZnCl2 : 70 ; NiCl2,6H2O : 25 ; CuCl2,2H2O : 15 ; NaMoO4,2H2O : 25 ; HCl : 1755) and 100mM of MES (2-[N-morpholino] ethane sulfonic acid buffer).

Glucose (Sigma), cellobiose (Fluka), arabinose (Sigma), xylose and xylan (Sigma) concentrations were fixed at 5 $g_{COD}.l^{-1}$ whereas micro-crystalline cellulose (MCC, Fluka) and wheat straw (Haussmann common wheat straw) were introduced at 10 $v_{olatile\ solid}.l^{-1}$ to increase the production of metabolites and remain above the detection limit of metabolites. Heat treated inoculum was then added to reach a substrate / inoculum (S/X) ratio of 10 $g_{COD\ substrate}.g^{-1}_{COD\ inoculum}$.

Volatile solid analysis of wheat straw and MCC were performed in quadriplicates according to the APHA standard methods (APHA, 1999). Chemical oxygen demand (COD) was analysed using Spectroquant® kit (Merk) according to manufacturer's indications.

After inoculation, bottles were sealed with a rubber stopper and locked with an aluminium screw. Head space was then purged with 0.2µm-filtered nitrogen gas to remove oxygen traces and keep the conditions anaerobic. The fermentation was stopped when the hydrogen production stabilized to avoid further consumption.

2.2. Metabolites and gas composition analysis

Gas production was monitored every 8 hours with an automatic micro-gas chromatograph (SRA µ-GC R3000) equipped with two columns: a Molsieve 10m/PPU at 80°C with Argon as vector gas and a VAR 8m/PPU at 70°C with Helium, for O_2-CH_4-H_2-N_2 and CO_2 analysis, respectively. The TCD temperature was set at 90°C.

Gas production was estimated by pressure measurement. From the gas composition and volume analysis, a modified Gompertz model was used to assess hydrogen production kinetic parameters (Eq. 1):

$$H(t) = Pexp\left\{-exp\left[\frac{Rm.e}{P}(\lambda - t) + 1\right]\right\} \quad (1)$$

Where H is the cumulative volume of hydrogen production (ml) along the incubation time (t), P is the maximum cumulative hydrogen production ($ml_{H2}.g^{-1}_{eq\ initial\ COD}$), Rm is the maximum hydrogen production rate ($ml_{H2}.g^{-1}_{eq\ initial\ COD}.d^{-1}$), λ is the lag phase (days) and e is exp(1). The values of P, Rm and λ were estimated using grofit R package (v 1.1.1-1) with nonlinear least square fitting (Kahm et al., 2010).

Soluble metabolites, i.e., volatile fatty acids (VFAs) and organic acids, solvents and residual sugars, were quantified before and after fermentation by Gas Chromatography (GC) and High Performance Liquid Chromatography (HPLC), respectively. Samples were filtrated at 0.2µm prior to analysis. The HPLC was coupled to refractometric detection (Waters R410). Chemicals were separated by an Aminex HPX-87H column (300 x 7.8mm, Biorad) equipped with a protective precolumn (Microguard cation H refill catbridges, Biorad). The eluting solution corresponded to 2 mM H_2SO_4 under a flow rate of 0.4 $ml.min^{-1}$. The column temperature was set at 35°C and the refractive index detector (Waters 2414) worked at 45°C. The gas chromatograph (GC 3900 Varian) was coupled to a flame ionization detector. Conditions were the same as previously described by Rafrafi *et al.* (2013). Measurements errors associated to µ-CG, GC and HPLC analysis were 1%, 5% and 3% respectively.

2.3. Characterisation of microbial community - DNA extraction, PCR amplification and sequencing

Ten mL of liquid sample were collected before and after the fermentation test. Samples were first centrifuged 10 min at 5,752g. After removing 8ml of the supernatant, the pellet was resuspended and aliquots of 500 µl were introduced in 4 sterile eppendorf tubes of 2 ml. The tubes were then centrifuged 5min at 16,662g. The pellets were finally stored at -20°C prior to DNA extraction. Cell lysis and DNA

extraction was performed according to manual instructions as previously described by Saur *et al* (2016). DNA purification was performed using the QIAamp DNA minikit (Qiagen, Hilden, Germany) according to manufacturer's instructions. Purified DNA was conserved at -20°C in 50 µl of molecular grade purity water until further use.

The V3 region of the 16S rRNA gene were amplified as presented before by Carmona-Martinez *et al* (2015). The PCR products were purified and loaded onto the Illumina MiSeq cartridge according to the manufacturer's instructions for sequencing of paired 300 bp reads (v3 chemistry). Library preparation and sequencing was done at the GeT PlaGe Sequencing Center of the Genotoul Lifescience Network in Toulouse, France.

A modified version of the Standard Operation Procedure for MiSeq data (Kozich et al., 2013) in Mothur version 1.35.0 (Schloss et al., 2009) was used to assemble forward and reverse sequences. Sequences were pre-clustered at 4 differences in nucleotides over the length of the amplicon and chimeras were checked using uchime (Edgar et al., 2011). Scarce sequences that appeared less than three times in the entire data-set were removed. Alignment and taxonomic affiliation from the 16S rRNA sequences was performed with SILVA SSU Ref NR99, release 119, as provided by Mothur (Schloss et al., 2009). Maximum of 44,503 and minimum of 14,941 sequences were obtained from the samples. 14,000 sequences with a mean length of 428 bp were considered per samples for data analysis. As shown in rarefaction curves (see supplementary materials) the number of selected sequences was enough to significantly represent the final communities. Rarefaction curves were drawn with the "*rarecurve()*" function of the *vegan* R package (Oksanen et al., 2016). Sequences have been submitted to GenBank with accession No. XXXXX.

2.4. Statistical data analysis

Principal component analysis (PCA) was performed on reduced and scaled data using the "*prcomp()*" function from the built-in R stats package. Graphic representation was performed using "*ggbiplot*" (Vu, 2011).

Bacterial community analysis was performed on unique Operational Taxonomic Units (OTUs). Principal Coordinate Analysis (PCoA) was performed on unique OTU after data transformation by the Hellinger method to avoid noise generated by highly minor OTUs. Hellinger transformation was performed with the "*decostand()*" function from the *vegan* R package (Oksanen et al., 2016) and PCoA with the "*pcoa()*" function in the ape package (Paradis et al., 2004).

The OTUs with relative abundance higher than 5% in at least one sample were selected to perform further analysis. The average of their relative abundance by replicate was presented as heatmap using the *"heatmap.2()"* function of the gplots R package (Warnes et al., 2016). Influence of major OTU identified on metabolites produced was analysed by the "*envfit()*" function(permutations 9999) which fit environmental vectors onto ordination, PCA done on major OTUs in this case (Oksanen et al., 2016)

3. Results and discussion

3.1. Hydrogen production performances

Gas production was periodically analysed until a hydrogen production plateau was observed. It was reached after 4.5, 6.4, 21.5, 6.5, 7.5, 8 and 14.6 days of fermentation for glucose, cellobiose, MCC, arabinose, xylose, xylan and wheat straw,

186 respectively. At this time, experiments were stopped to avoid changes in metabolism
187 due to hydrogen consumption. No methane production was observed during the
188 experiment showing that the heat shock pre-treatment totally supressed the
189 methanogenic activity for the time of experiment.
190 Dynamics of hydrogen production along the experiment are shown in Figure 1.
191 Hydrogen production data were fitted to a modified Gompertz model with a
192 determination of coefficient (R^2) up to 0.99 and the model parameters are presented in
193 Table 1. Maximum of cumulated hydrogen production (P) on glucose was 31±12
194 $ml_{H2}.g^{-1}_{eq.initial\ COD}$ which was almost a third higher than cellobiose and MCC, two
195 polymers of glucose. The average maximum hydrogen production yield was also
196 different between cellobiose and MCC with 23 and 12 $ml_{H2}.g^{-1}_{eq.initial\ COD}$ obtained
197 respectively. In accordance with the degree of polymerisation, hydrogen production rate
198 (Rm) was also different between hexose-based susbstrates since 29±12 $ml_{H2}.g^{-1}_{eq.initial}$
199 $_{COD}.d^{-1}$ were obtained on glucose and 12±1 and 1.5±0.6 $ml_{H2}.g^{-1}_{eq.initial\ COD}.d^{-1}$ were
200 calculated for cellobiose and cellulose, respectively. Lag phase (λ) was similarly
201 impacted since it was 12 days for MCC but only 2 days for glucose and cellobiose.
202 Consistently, several authors showed that the production of hydrogen depends
203 on the degree of polymerisation of the carbohydrates (Danilenko et al., 1993; Monlau et
204 al., 2012a; Quéméneur et al., 2012; Sambusiti et al., 2013). Indeed, a hydrolysis step of
205 carbohydrate polymers is required to produce simpler molecules that can further enter
206 into microbial cells prior to be metabolized. This step impacts directly the bioprocess
207 kinetics (Kumar et al., 2009). However hydrolysis requires also energy in the forms of
208 ATP and NADH equivalents that reduces final hydrogen production. Therefore, high

hydrogen yields are usually observed in presence of high soluble sugars-content substrates as previously reported (Guo et al., 2014; Monlau et al., 2012b).

The modified Gompertz model parameters were also estimated for pentose-based substrates. The C5 substrates showed higher hydrogen yields than C6 substrates, when comparing substrates with equivalent polymerisation degree. As an illustration, the fermentation of arabinose and xylose led to an increase of the P_{max} value of 2 and 3 times when compared to glucose, respectively. The maximum hydrogen production rate Rm was also higher with 32 and 40 $ml_{H2}.g^{-1}_{eq.initial\ COD}.d^{-1}$ for arabinose and xylose, respectively.

These results suggest that pentoses are preferred carbon sources for the production of hydrogen using this inoculum and under these experimental conditions. Such effect was already reported by Prakasham *et al*. (2009) who used a mixed inoculum developed in buffalo dung compost, although the reported differences between hexose and pentose substrates were lower than in the present study. Mäkinen *et al.*(2012) also obtained the same trend with hot spring culture. All these observations suggest that the metabolic pathway is strongly dependent on the origin of the inoculum especially when considering monomeric carbohydrates. Indeed, the fermentative community developed here is more favourable to produce hydrogen from C5 than from C6.

With C5 substrates, the polymerisation degree had also a negative effect on the overall hydrogen production performances, since lower P and Rm and higher λ were observed for xylan than with xylose.

In the case of wheat straw as model material of complex lignocellulosic biomass, the complex structure led to very poor hydrogen value which is coherent to

233 literature (Agbor et al., 2011). Similarly to micro-crystalline cellulose, only 8% of the
234 initial equivalent COD was converted with a very low hydrogen value.
235 However, when comparing the quantity of hydrogen produced per unit of COD
236 converted during the process, i.e. hydrogen production yield (Table 1), it could be
237 observed that more consumed COD was transformed into hydrogen for MCC and
238 cellobiose than observed for glucose, with 8, 4.2 and 1.7 $mmol_{H2}.g^{-1}_{eq.COD\ consumed}$
239 measured respectively. Hence, even if the degradation was weaker on cellobiose and
240 MCC than on glucose, the metabolisms of the flora converting the polymer seems to be
241 oriented to the production of hydrogen contrary to what observed on glucose.
242 In summary, the hydrogen production correlated well with both the degree of
243 polymerisation and the type of residual sugars (C5 or C6). When considering the
244 relative amount of COD converted to H_2, cumulated hydrogen ranged from 11 to 2%
245 only. This result should be compared to a theoretical value of 21% for mixed cultures,
246 as suggested by Hawkes *et al*. (2007). Therefore, the other metabolites co-produced
247 during fermentation were also considered.

248 **3.2. Other fermentation metabolites**

249 Soluble fermentation products were analysed at the end of batch tests. Amounts
250 of metabolites were expressed in $mg_{\ product\ eq.\ COD}.g^{-1}_{\ initial\ substrate\ eq.COD}$ and are presented
251 in Table 2. A principal component analysis (PCA) was carried out to illustrate the
252 variability in metabolic pathways between the different substrates (Figure 2).
253 The COD conversion was evaluated by COD balance according to the
254 metabolites measured. Because batch tests were stopped at the maximum of hydrogen
255 production, the initial substrate COD was not necessarily fully converted at the end of
256 the experiment. In particular, the percentage of COD converted at the final time

decreased from 79±3 to 4.68±0.03 according to the degree of polymerisation for C6 substrates. Indeed, the compact structure of micro-crystalline cellulose is an obstacle for hydrolytic enzymes to access substrate linkage. Complex substrates may not be fully converted at the end of the process as it could be observed in this study (Kumar et al., 2009).

Like for hexose substrates, the COD converted at the end of the pentose fermentation was higher for the monomer than for the polymer which supports that the degree of polymerisation also has an impact regardless the sugar residue.

The use of xylose and arabinose as different C5 isomer (on carbon 2) showed different conversion yields since only 44% of the initial COD was converted under the form of metabolites for arabinose against 64.4% for xylose. Conversion of arabinose and xylose implies the use of different enzymes. L-arabinose is first converted by via L-arabinose isomerase, L-ribulokinase and L-ribulose-5-P 4- epimerase to L-ribulose, L-ribulose-5- phosphate and D-xylulose-5-phosphate respectively, whereas D-xylose is directly transformed into D-xylulose by D-xylose isomerase (Bettiga et al., 2009). Hence depending on their enzymatic potential, bacteria will have the ability to converted one pentose, the other or both.

Metabolic patterns appear to be strongly linked to the type of carbohydrates (C6 or C5). Hexoses (glucose and cellobiose) were mainly converted into lactate (>70%). The low hydrogen yield was likely linked to the low production of butyrate as second main metabolite, as previously suggested by Guo *et al*. (2014). Acetate and ethanol represent less than 10% of all the metabolites produced. However, the proportion of acetate and butyrate produced was higher for the polymers of glucose than observed for the monomer. This metabolic pattern favourable to the production of hydrogen might

explain the high value of hydrogen production yield observed in Table 1 for cellobiose and MCC.

For C5 fermentation (xylose and arabinose), metabolisms were different since very low amount of lactate accumulated for arabinose, and butyrate was the main metabolic pathway (30%). Consistently, hydrogen yield was higher than with hexose. Similar results have been observed in a previous study. Using hot spring culture as fermentative microorganism source, Mäkinen *et al.*(2012) showed that lactate was preferentially produced during glucose conversion as observed in this study. Interestingly, pentose was converted into butyrate but also formate, metabolite unfound there.

Ethanol and acetate were produced in higher quantity from C5 than from C6 (x10) and a new metabolite, isobutyrate, was identified. To the authors' knowledge, no information about isobutyrate production from pentose-based sugars is available in the literature. However, the conversion into ethanol has been largely studied in the field of biofuel production. Even if yeast is the main microorganism studied, bacteria are also able to produce bio-ethanol (Bettiga et al., 2009).

Moreover, identification of different by-products depending on the pentose sugar is observed. While lactate was more produced during arabinose conversion, propionate was specific of xylose and xylose-based polymers. Indeed, bacteria did not have the same ability to convert the two pentoses as explained before.

3.3. Strong selection in microbial communities

The differences in metabolic patterns observed for each substrate might be the consequence of different metabolic pathways within the same microbial community or to the selection of specific bacterial communities. Therefore, bacterial DNA was

extracted from each sample and the V3 region of the RNA 16S ribosomal region was amplified and sequenced by high-throughput amplicon sequencing. Principal coordinate analysis (PCoA) was used to represent the euclidean distance separating each final community (Figure 3).

First, it was observed that samples can be distinguished on the first axis according to the polymerisation degree. Communities growing on monomers and dimers are located on the left side whereas polymers-based communities, including wheat straw, are on the right side. The second axis was more related to the carbon content of the substrate. Similarly to the metabolic patterns, it can be concluded that the final bacterial structure was dependent on both the polymerisation degree and the type of substrate.

The relative proportion of the major OTUs (relative abundance > 5%) found for each substrate are presented in Figure 4. Main OTUs were affiliated to the *Clostridiaceae*, *Bacillaceae* and *Peanibacillaceae* families when both pentose and hexose simple sugars were used as substrate (xylose, arabinose, glucose and cellobiose). These bacteria have been well described in mixed cultures fermentation. More particularly, members of the *Clostridiaceae* family have generally been associated to hydrogen production, while *Bacillaceae* and *Peanibacillaceae* are involved in lactic acid fermentation (Ghimire et al., 2015).

Interestingly, these major OTUs were not found in the reactors containing complex substrates such as xylan, cellulose and wheat straw. Here, identified bacteria were affiliated to the *Ruminoccocaceae* family only. Bacteria belonging to this family can be related to *Clostridium* bacteria and are mainly microorganisms found in rumen, reported as efficiently degrading complex biomass (Hung et al., 2011). Because

329 *Ruminococcaceae* bacteria were not found in reactors fed with simple substrates, this
330 suggests that *Clostridiaceae*, *Bacillaceae* and *Paenibacillaceae* are more competitive
331 with regards to readily biodegradable sugars. In counterpart, the hydrolytic activity of
332 the *Ruminococcaceae* confers to them an ecological advantage to grow on more
333 complex organic materials.

334 Three proteobacteria were also identified in reactors fed with complex
335 substrates. The OTU56 affiliated to the *Burkholderia* genus was present in MCC-based
336 reactors. Similar bacteria were already described for their hydrolytic activity during
337 complex organic biomass degradation (Mohana et al., 2008). Their presence was often
338 associated to the production of hydrogen (Porwal et al., 2008).

339 The OTU7 and OTU199 found in xylan-based reactors were both affiliated to
340 the *Klebsiella* genus (Wong et al., 2014). These facultative anaerobes were previously
341 reported as efficient hydrogen producers. However, they exhibit a concomitant ethanol
342 pathway which may explain the high proportion of ethanol (25±6%) found in these
343 reactors (De Amorim et al., 2012).

344 Metabolites measured at the end of fermentation were fitted onto ordination
345 done with main OTUs to estimate the correlation strength existing between microbial
346 communities and metabolisms. Results show that acetate and lactate correlated better
347 with bacterial community structures than other metabolites (<0.1% of significance,
348 Figure 5). Hence, the production of acetate seems to be explained by the presence of
349 OTU9 and OTU26 affiliated to *Clostridium sp.* and OTU12 and OTU29 affiliated to
350 *Paenibacillus sp.* developed in C5-based sugar reactors. With lesser significance (<1%
351 and 5%), the emergence of these bacteria also correlated with hydrogen, butyrate and
352 ethanol production.

353 Lactate production is represented by the presence of OTU18 (*Paenibacillus sp.*),
354 OTU47 (*Clostridium sp.*) which were mainly identified in hexose-based reactors.
355 Interestingly, OTU11 (*Clostridium sp.*), OTU9 and OTU20 affiliated to *Bacillus sp.* are
356 located at in the hexose substrate zone although they are present in both C6 and C5
357 based reactors. *Bacillus sp.* are facultative anaerobes specially essential at the begging
358 of the fermentation since they allow anaerobic condition by consuming residual oxygen
359 (Huang et al., 2010). Their ability to grow on many carbohydrates may explain their
360 presence in both hexose and pentose-based reactors (Stülke and Hillen, 2000).
361 Few studies also showed that the type of substrate could impact the bacterial
362 community structure (Akutsu et al., 2009; Cheng et al., 2011; Li and Chen, 2007; Qiu et
363 al., 2016; Quéméneur et al., 2011). Table 3 reports hydrogen production yields observed
364 in literature using different bacterial cultures and various substrates. In all cases, acetate
365 and butyrate were the main metabolites observed, which was accompanied with higher
366 hydrogen production yields than measured in the present work. Bacteria affiliated to
367 *Clostridium* sp. were identified as main microorganisms composing the mixed culture
368 whereas in the present study, *Bacillus* sp. and *Paenibacillus* sp. represented a large part
369 of the communities. These differences in structures of the bacterial communities led in
370 this case to the production of lactate as main metabolite from hexose-based substrates.
371 Hence, depending on the residue used, bacterial community developed different
372 structures at the end of the fermentation that drove the metabolism to lactate or
373 acetate/butyrate production. Selection of bacteria represents an ecological advantage
374 which favours the development of microorganisms on specific substrate. However, this
375 sensitivity of bacterial communities structure to substrate composition should be taken
376 into consideration when using continuous systems (Bakonyi et al., 2014). By controlling

the substrate input, it could be easier to maintain the community structure in the reactor and, thus, the performance stability for hydrogen production. This could also lead to improve the biomass conversion yield by selecting specific bacteria able to degrade a complex substrate. The use of biological strategies to increase organic matter conversion into biohydrogen has already been performed in dark fermentation (Kotay and Das, 2009; Kuo et al., 2012). Illustratively, the addition of keystone species into the medium as those identified in this study could be a solution to improve the production of hydrogen from lignocellulosic residues (Rafrafi et al. 2013).

4. Conclusion

This study shows that fermentative hydrogen yields from model carbohydrates was linked to the type of sugars (pentose or hexose) and the degree of polymerisation. Hydrogen production was strongly linked to a specific selection of bacterial community structures with different metabolic patterns. Species affiliated to *Paenibacillus sp.*, *Bacillus sp.* were associated to lactate production from hexoses, whereas *Clostridium sp.* were dominant in hydrogen-producing reactors fed with pentoses. The presence of *Ruminococcaceae sp.* on polymeric sugars (cellulose, xylan and wheat straw) suggests that these bacteria play an important role in the hydrolytic activity.

Acknowledgements

The authors thank Camille Demblon and Anais Bonnafous for technical supports.

This work was funded by the National Institute of Agronomic Research and the agronomic school Montpellier SupAgro.

Genomic analysis was performed by the GeT PlaGe Sequencing Center of the Genotoul Lifescience Network in Toulouse, France.

References

1. Agbor, V.B., Cicek, N., Sparling, R., Berlin, A., Levin, D.B., 2011. Biomass pretreatment: Fundamentals toward application. Biotechnol. Adv. 29, 675–685.
2. Akutsu, Y., Lee, D.-Y., Li, Y.-Y., Noike, T., 2009. Hydrogen production potentials and fermentative characteristics of various substrates with different heat-pretreated natural microflora. Int. J. Hydrogen Energy 34, 5365–5372.
3. APHA, 1999. Standard Methods for the Examination of Water and Wastewater, 20th ed.
4. Bakonyi, P., Nemestóthy, N., Simon, V., Bélafi-Bakó, K., 2014. Review on the start-up experiences of continuous fermentative hydrogen producing bioreactors. Renew. Sustain. Energy Rev. 40, 806–813.
5. Bettiga, M., Bengtsson, O., Hahn-Hägerdal, B., Gorwa-Grauslund, M.F., 2009. Arabinose and xylose fermentation by recombinant Saccharomyces cerevisiae expressing a fungal pentose utilization pathway. Microb. Cell Fact. 8, 40.
6. Cai, G., Jin, B., Monis, P., Saint, C., 2011. Metabolic flux network and analysis of fermentative hydrogen production. Biotechnol. Adv. 29, 375–387.
7. Carmona-Martínez, A.A., Trably, E., Milferstedt, K., Lacroix, R., Etcheverry, L., Bernet, N., 2015. Long-term continuous production of H2 in a microbial electrolysis cell (MEC) treating saline wastewater. Water Res. 81, 149–156.
8. Cheng, J., Su, H., Zhou, J., Song, W., Cen, K., 2011. Microwave-assisted alkali pretreatment of rice straw to promote enzymatic hydrolysis and hydrogen production in dark- and photo-fermentation. Int. J. Hydrogen Energy 36, 2093–2101.

9. Danilenko, A.N., Bogomolov, A.A., Yuryev, V.P., Dianova, V.T., Bogatyrev, A.N., 1993. Effect of the Polymerization Degree, Moisture Content, and Temperature on Kinetics of Hydrolysis of Corn Starch by Alpha-Amylase. Starch - Stärke 45, 63–65.
10. De Amorim, E.L.C., Sader, L.T., Silva, E.L., 2012. Effect of substrate concentration on dark fermentation hydrogen production using an anaerobic fluidized bed reactor. Appl. Biochem. Biotechnol. 166, 1248–1263.
11. Edgar, R.C., Haas, B.J., Clemente, J.C., Quince, C., Knight, R., 2011. UCHIME improves sensitivity and speed of chimera detection. Bioinformatics 27, 2194–2200.
12. Ghimire, A., Frunzo, L., Pirozzi, F., Trably, E., Escudie, R., Lens, P.N.L., Esposito, G., 2015. A review on dark fermentative biohydrogen production from organic biomass: Process parameters and use of by-products. Appl. Energy 144, 73–95.
13. Guo, X.M., Trably, E., Latrille, E., Carrere, H., Steyer, J.-P., 2014. Predictive and explicative models of fermentative hydrogen production from solid organic waste: Role of butyrate and lactate pathways. Int. J. Hydrogen Energy 39, 7476–7485.
14. Guo, X.M., Trably, E., Latrille, E., Carrère, H., Steyer, J.-P., 2010. Hydrogen production from agricultural waste by dark fermentation: A review. Int. J. Hydrogen Energy 35, 10660–10673.
15. Hawkes, F., Hussy, I., Kyazze, G., Dinsdale, R., Hawkes, D., 2007. Continuous dark fermentative hydrogen production by mesophilic microflora: Principles and progress. Int. J. Hydrogen Energy 32, 172–184.
16. Huang, Y., Zong, W., Yan, X., Wang, R., Hemme, C.L., Zhou, J., Zhou, Z., 2010. Succession of the bacterial community and dynamics of hydrogen producers in a hydrogen-producing bioreactor. Appl. Environ. Microbiol. 76, 3387–3390.
17. Hung, C.-H., Chang, Y.-T., Chang, Y.-J., 2011. Roles of microorganisms other than Clostridium and Enterobacter in anaerobic fermentative biohydrogen production

448 systems – A review. Bioresour. Technol. 102, 8437–8444.
449 18. Kahm, M., Kahm, M., Hasenbrink, G., Lichtenberg-Frate, H., Ludwig, J., Kschischo, M.,
450 2010. Grofit: Fitting biological growth curves. Nat. Preced. 33, 1–21.
451 19. Kalia, V.C., Purohit, H.J., 2008. Microbial diversity and genomics in aid of bioenergy. J.
452 Ind. Microbiol. Biotechnol. 35, 403–419.
453 20. Kleerebezem, R., van Loosdrecht, M.C., 2007. Mixed culture biotechnology for
454 bioenergy production. Curr. Opin. Biotechnol. 18, 207–212.
455 21. Kotay, S.M., Das, D., 2009. Novel dark fermentation involving bioaugmentation with
456 constructed bacterial consortium for enhanced biohydrogen production from
457 pretreated sewage sludge. Int. J. Hydrogen Energy 34, 7489–7496.
458 22. Kozich, J.J., Westcott, S.L., Baxter, N.T., Highlander, S.K., Schloss, P.D., 2013.
459 Development of a dual-index sequencing strategy and curation pipeline for analyzing
460 amplicon sequence data on the miseq illumina sequencing platform. Appl. Environ.
461 Microbiol. 79, 5112–5120.
462 23. Kumar, P., Kumar, P., Barrett, D.M., Barrett, D.M., Delwiche, M.J., Delwiche, M.J.,
463 Stroeve, P., Stroeve, P., 2009. Methods for Pretreatment of Lignocellulosic Biomass for
464 Ef cient Hydrolysis and Biofuel Production. Ind. Eng. Chem. Analytical Ed. 3713–3729.
465 24. Kuo, W.-C., Chao, Y.-C., Wang, Y.-C., Cheng, S.-S., 2012. Bioaugmentation Strategies to
466 Improve Cellulolytic and Hydrogen Producing Characteristics in CSTR Intermittent Fed
467 with Vegetable Kitchen Waste and Napiergrass. Energy Procedia 29, 82–91.
468 25. Li, D., Chen, H., 2007. Biological hydrogen production from steam-exploded straw by
469 simultaneous saccharification and fermentation. Int. J. Hydrogen Energy 32, 1742–
470 1748.
471 26. Mäkinen, A.E., Nissilä, M.E., Puhakka, J.A., 2012. Dark fermentative hydrogen
472 production from xylose by a hot spring enrichment culture. Int. J. Hydrogen Energy 37,

12234–12240.

27. Menon, V., Rao, M., 2012. Trends in bioconversion of lignocellulose: Biofuels, platform chemicals & biorefinery concept. Prog. Energy Combust. Sci. 38, 522–550.
28. Mohana, S., Shah, A., Divecha, J., Madamwar, D., 2008. Xylanase production by *Burkholderia* sp. DMAX strain under solid state fermentation using distillery spent wash. Bioresour. Technol. 99, 7553–7564.
29. Monlau, F., Barakat, A., Steyer, J.P., Carrere, H., 2012a. Comparison of seven types of thermo-chemical pretreatments on the structural features and anaerobic digestion of sunflower stalks. Bioresour. Technol. 120, 241–7.
30. Monlau, F., Sambusiti, C., Barakat, A., Guo, X.M., Latrille, E., Trably, E., Steyer, J.-P., Carrere, H., 2012b. Predictive Models of Biohydrogen and Biomethane Production Based on the Compositional and Structural Features of Lignocellulosic Materials. Environ. Sci. Technol. 46, 12217–12225.
31. Nissilä, M.E., Lay, C.-H., Puhakka, J. a., 2014. Dark fermentative hydrogen production from lignocellulosic hydrolyzates – A review. Biomass and Bioenergy 67, 145–159.
32. Oksanen, J., Blanchet, F.G., Kindt, R., Legendre, P., Minchin, P.R., O'Hara, R.B., Simpson, G.L., Solymos, P., Stevens, M.H.H., Wagner, H., 2016. vegan: Community Ecology Package. R package version 2.3-3. http://CRAN.R-project.org/package=vegan.
33. Paradis, E., Claude, J., Strimmer, K., 2004. APE: Analyses of Phylogenetics and Evolution in R language. Bioinformatics 20, 289–290.
34. Porwal, S., Kumar, T., Lal, S., Rani, A., Kumar, S., Cheema, S., Purohit, H.J., Sharma, R., Singh Patel, S.K., Kalia, V.C., 2008. Hydrogen and polyhydroxybutyrate producing abilities of microbes from diverse habitats by dark fermentative process. Bioresour. Technol. 99, 5444–5451.
35. Qiu, C., Zheng, Y., Zheng, J., Liu, Y., Xie, C., Sun, L., 2016. Mesophilic and Thermophilic

Biohydrogen Production from Xylose at Various Initial pH and Substrate Concentrations with Microflora Community Analysis. Energy & Fuels 30, 1013–1019.

36. Quéméneur, M., Hamelin, J., Barakat, A., Steyer, J.-P., Carrère, H., Trably, E., 2012. Inhibition of fermentative hydrogen production by lignocellulose-derived compounds in mixed cultures. Int. J. Hydrogen Energy 37, 3150–3159.
37. Quéméneur, M., Hamelin, J., Benomar, S., Guidici-Orticoni, M.-T., Latrille, E., Steyer, J.-P., Trably, E., 2011. Changes in hydrogenase genetic diversity and proteomic patterns in mixed-culture dark fermentation of mono-, di- and tri-saccharides. Int. J. Hydrogen Energy 36, 11654–11665.
38. Rafrafi, Y., Trably, E., Hamelin, J., Latrille, E., Meynial-Salles, I., Benomar, S., Giudici-Orticoni, M.-T., Steyer, J.-P., 2013. Sub-dominant bacteria as keystone species in microbial communities producing bio-hydrogen. Int. J. Hydrogen Energy 38, 4975–4985.
39. Saady, N.M.C., 2013. Homoacetogenesis during hydrogen production by mixed cultures dark fermentation: Unresolved challenge. Int. J. Hydrogen Energy 38, 13172–13191.
40. Sambusiti, C., Monlau, F., Ficara, E., Carrère, H., Malpei, F., 2013. A comparison of different pre-treatments to increase methane production from two agricultural substrates. Appl. Energy 104, 62–70.
41. Saratale, G.D., Chen, S., Lo, Y., Saratale, R.G., Chang, J., 2008. Outlook of biohydrogen production from lignocellulosic feedstock using dark fermentation – a review. J. Sci. Ind. Res. 67, 962–979.
42. Saur, T., Escudié, R., Santa-Catalina, G., Bernet, N., Milferstedt, K., 2016. Conservation of acquired morphology and community structure in aged biofilms after facing environmental stress. Water Res. 88, 164–172.

523 43. Schloss, P.D., Westcott, S.L., Ryabin, T., Hall, J.R., Hartmann, M., Hollister, E.B.,
524 Lesniewski, R.A., Oakley, B.B., Parks, D.H., Robinson, C.J., Sahl, J.W., Stres, B.,
525 Thallinger, G.G., Van Horn, D.J., Weber, C.F., 2009. Introducing mothur: Open-source,
526 platform-independent, community-supported software for describing and comparing
527 microbial communities. Appl. Environ. Microbiol. 75, 7537–7541.
528 44. Stülke, J., Hillen, W., 2000. Regulation of Carbon Catabolism in Bacillus Species. Annu.
529 Rev. Microbiol. 54, 849–880.
530 45. UNFCCC. Conference of the Parties (COP), 2015. Adoption of the Paris Agreement.
531 Proposal by the President., in: Paris Climate Change Conference - November 2015, COP
532 21. Paris, p. 32.
533 46. Vu, V.Q., 2011. ggbiplot: A ggplot2 based biplot. R package version 0.55.
534 http://github.com/vqv/ggbiplot.
535 47. Wang, J., Wan, W., 2009. Factors influencing fermentative hydrogen production: A
536 review. Int. J. Hydrogen Energy 34, 799–811.
537 48. Warnes, G.R., Bolker, B., Bonebakker, L., Gentleman, R., Huber, W., Liaw, A., Lumley,
538 T., Maechler, M., Magnusson, A., Moeller, S., Schwartz, M., Venables, B., 2016.
539 Package " gplots ", Various R Programming Tools for Plotting Data.
540 49. Wong, Y.M., Wu, T.Y., Juan, J.C., 2014. A review of sustainable hydrogen production
541 using seed sludge via dark fermentation. Renew. Sustain. Energy Rev. 34, 471–482.
542 50. Zhang, B., He, P.-J., Lü, F., Shao, L.-M., Wang, P., 2007. Extracellular enzyme activities
543 during regulated hydrolysis of high-solid organic wastes. Water Res. 41, 4468–78.
544

Figure captions

Figure 1: Production of hydrogen analysed for each substrate during the experiment ml_{H2}.g-1 of initial substrate eq.COD for a) glucose (●), cellobiose (●), arabinose (●), xylose (●), xylan (●), and wheat straw (●), and b) for MCC (●).Error bars correspond to standard deviation observed between each replicate.

Figure 2: Principal component analysis done on metabolite production. Symbols correspond to each substrate, Glucose (⬢), Cellobiose (□), Microcrystalline cellulose (●), Arabinose (△), Xylose (▽), Xylan (◇) and Wheat Straw (☆).

Figure 3: Principal coordinate analysis (PCoA) done on OTUs after Hellinger transformation. Symbols correspond to each substrate, Glucose (⬢), Cellobiose (□), Microcrystalline cellulose (●), Arabinose (△), Xylose (▽), Xylan (◇) and Wheat Straw (☆).

Figure 4: Major OTUs identified in reactors for each substrate (relative abundance >5%). White colour corresponds to absence of identified OTU, light blue a low relative abundance, and black relative abundance close to the maximum measured (38%).

Figure 5: Principal component analysis ordination plot of major bacteria composing the sample bacterial community (a) with metabolite variables as predictors onto the ordination (b) analysed by the *envfit* function (permutations 9999, R package *vegan*). Symbols correspond to substrates: Glucose (⬢), Cellobiose (□), Microcrystalline cellulose (●), Arabinose (△), Xylose (▽), Xylan (◇) and Wheat Straw (☆); and to number of Operation Taxonomic Unit (OTU, ✚). Stars following metabolite name represent the significance of the fit (***<0.001; **<0.01, *<0.05).

Table 1: Kinetic parameters of hydrogen production in batch tests according to the initial substrate concentration determined from modified Gompertz equation with P the maximum cumulative hydrogen production (mlH2.g-1eq initial COD), Rm the maximum hydrogen production rate (mlH2.g-1eq initial COD.d-1), λ the lag phase (days) and R^2 the coefficient of determination of the model. Values correspond to the average of four replicates ± standard deviation observed between these replicates. Values in % in the H2 yield column correspond to the proportion of the maximum theoretical value suggested by Hawkes et al. (2007), i.e 2.5 molH2.mol-1 degraded substrate in glucose equivalent.

Table 2: Metabolites accumulated at the end of the fermentation tests (in mg $_{\text{product eq. COD}}.g_{\text{initial substrate eq. COD}}^{-1}$.) Values correspond to the average of four replicates ± standard deviation. Values in italic and in parenthesis correspond to the proportion (in %) of each product among all the metabolites produced in a same batch test ± standard deviation.

Table 3: Hydrogen yields, metabolic patterns and main identified bacteria obtained from dark fermentation performed on different inocula and substrates in the literature. Units of hydrogen yield, H_2 column, correspond to a) $mol_{H2}.mol^{-1}_{substrate}$, b) $mmol_{H2}.g^{-1}_{VS}$, c) $mmol_{H2}.g^{-1}_{substrate}$, d) $mmol_{H2}.g^{-1}_{TVS}$ and e) $mmol_{H2}./g^{-1}_{DCO}$. Metabolites are expressed in % of COD converted and abbreviations correspond to Acetate (HAc), Butyrate (HBut); Caproate (HCap), Ethanol (EtOH), Lactate (HLac), Propionate (Hpr), Formate (Hfor), Valerate (HVal) and Succinate (HSuc).

Figure

Click here to download Figure: FIG1.pptx

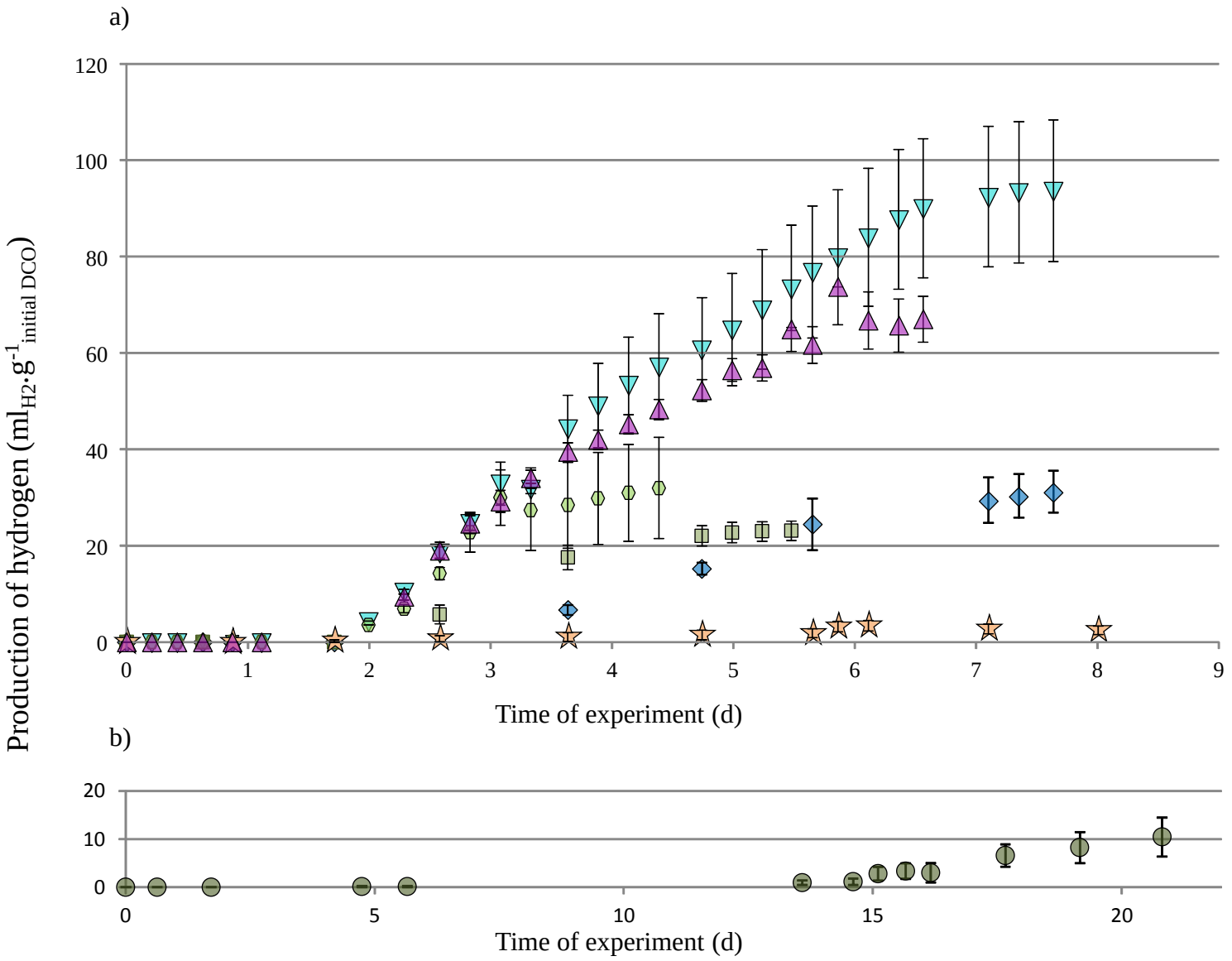

Figure

Click here to download Figure: FIG2.pptx

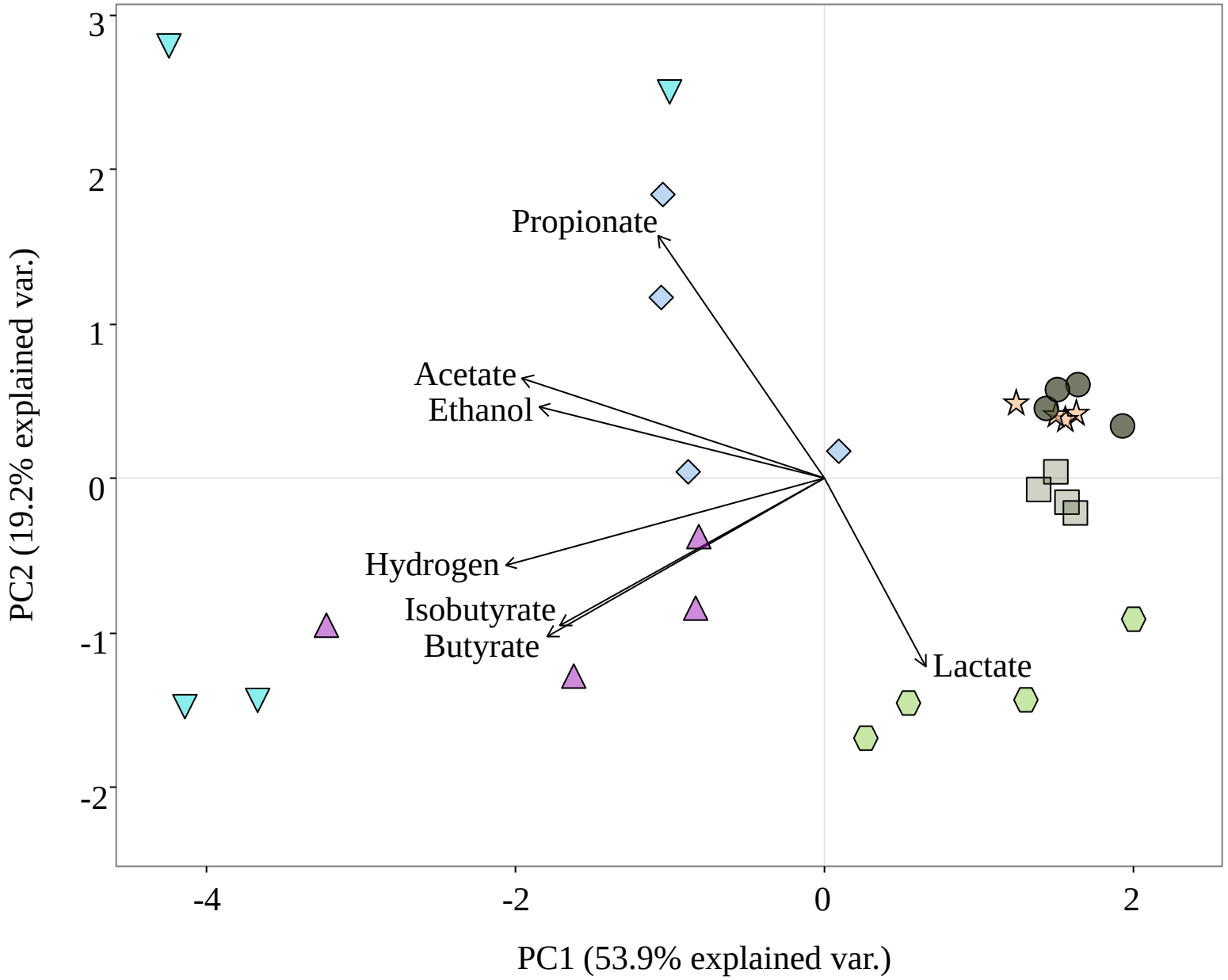

Figure

Click here to download Figure: FIG3.pptx

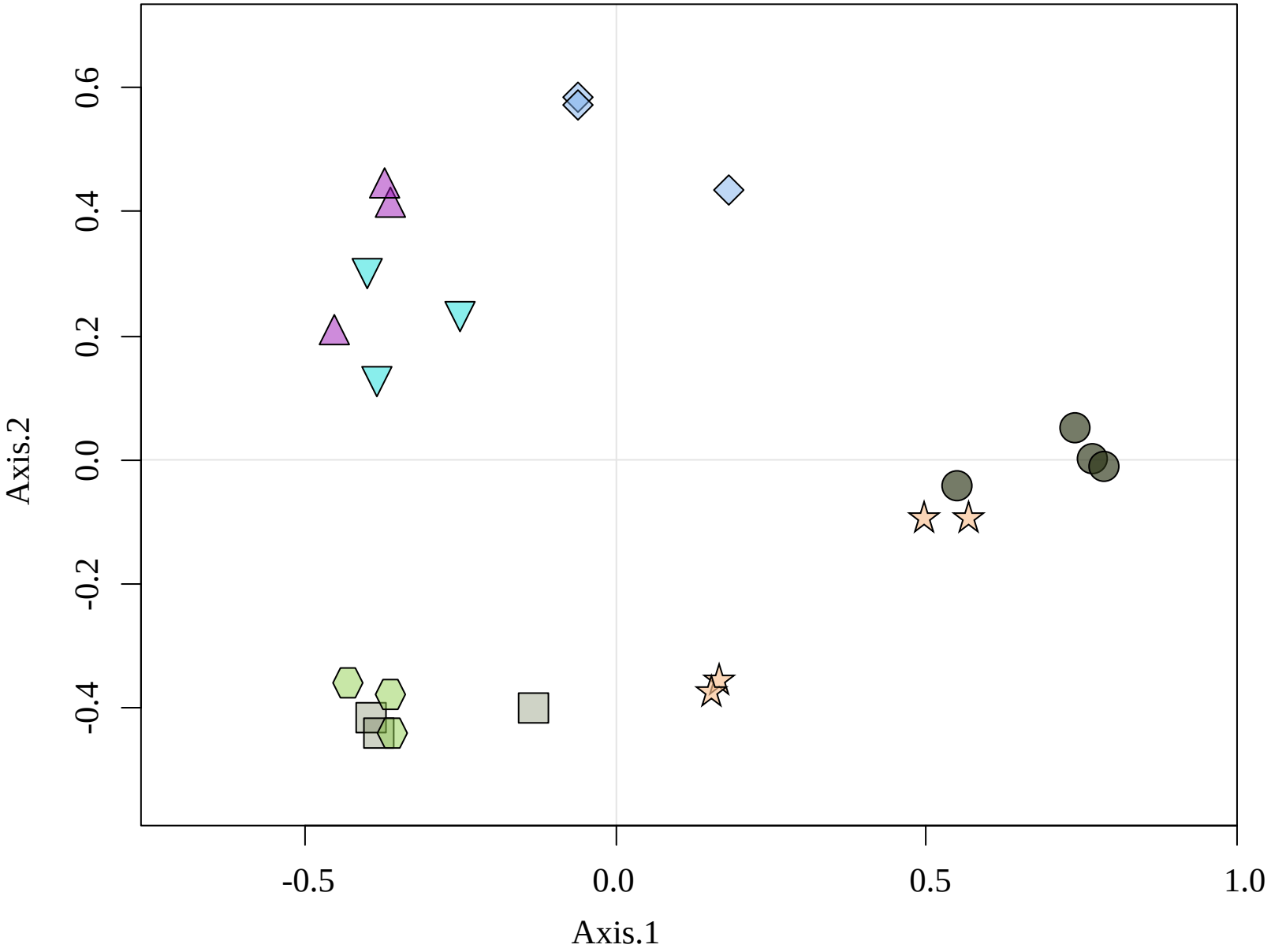

Figure

Click here to download Figure: FIG4.pptx

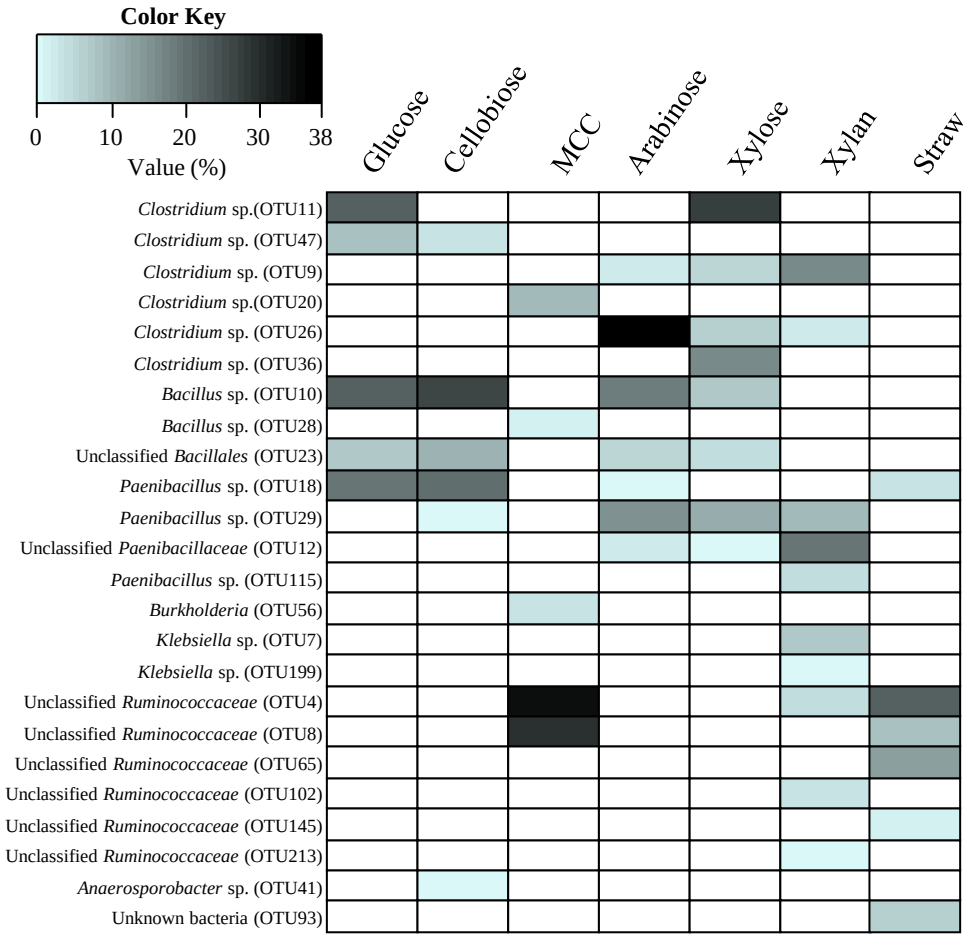

Figure

Click here to download Figure: FIG5.pptx

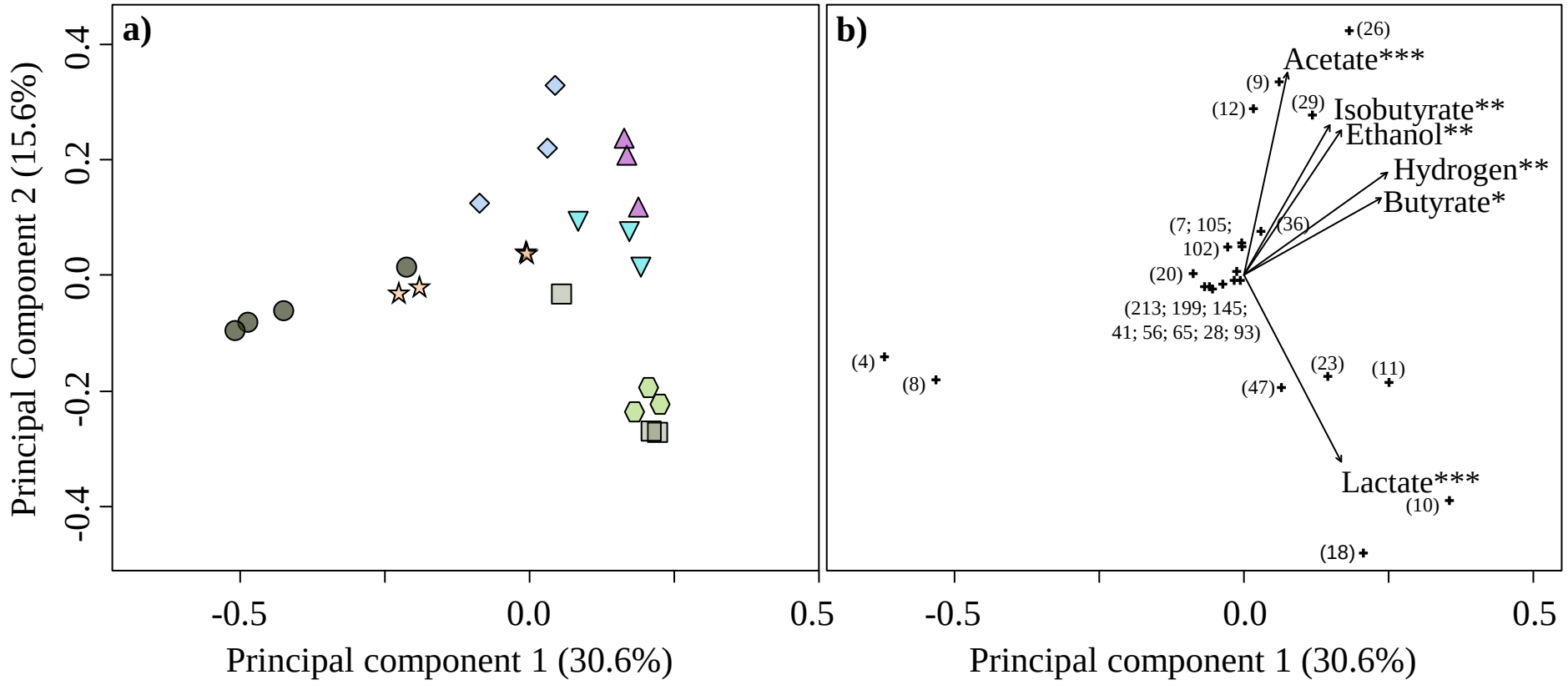

Table

Table 1: Kinetic parameters of hydrogen production in batch tests according to the initial substrate concentration determined from modified Gompertz equation with P the maximum cumulative hydrogen production (mlH2.g-1eq initial COD), Rm the maximum hydrogen production rate (mlH2.g-1eq initial COD.d-1), λ the lag phase (days) and R^2 the coefficient of determination of the model. Values correspond to the average of four replicates ± standard deviation observed between these replicates. Values in % in the H2 yield column correspond to the proportion of the maximum theoretical value suggested by Hawkes et al. (2007), i.e 2.5 molH2.mol-1 degraded substrate in glucose equivalent.

Substrate	Gompertz equation parameter values				H_2 yield (mmolH2.g eq. COD consumed)
	P ($ml_{H2}.g^{-1}_{eq.COD\ initial}$)	Rm ($ml_{H2}.g^{-1}_{eq.COD\ initial}.d^{-1}$)	λ (days)	R^2	
Glucose	31±12	29±12	1.9±0.2	0.999±0.001	1.7±0.6 (13±5 %)
Cellobiose	23±2	12±1	2.1±0.2	0.999±0.001	4.2±0.6 (32±4 %)
Cellulose	12±5	1.5±0.6	12.1±0.5	0.997±0.004	8±4 (62±31 %)
Arabinose	67±6	32±4	2.04±0.06	0.999±0.001	6.4±0.4 (49±3 %)
Xylose	94±17	40±11	2.4±0.3	0.999±0.001	6±1 (44±8 %)
Xylan	32±5	1±4	3.2±0.2	0.999±0.001	4.1±0.6 (31±5 %)
Straw	10±9	13±13	3±1	0.998±0.002	1.3±0.6 (10±4 %)

Table

Table 2: Metabolites accumulated at the end of the fermentation tests (in mg product eq. COD.ginitial substrate eq. COD-1.) Values correspond to the average of four replicates ± standard deviation. Values in italic and in parenthesis correspond to the proportion (in %) of each product among all the metabolites produced in a same batch test ± standard deviation.

Sample	Acetate	Butyrate	Isobutyrate	Propionate	Lactate	Ethanol	Hydrogen	COD converted (%)
Glucose	20±8 *(2.4±0.9)*	116±42 *(14±5)*	/	/	592±11 *(76±6)*	44±4 *(5.5±0.4)*	21±8 *(2.5±0.9)*	79±3
Cellobiose	11±4 *(5±2)*	11±11 *(5±5)*	/	/	165±12 *(73±2)*	23±3 *(11±1)*	15±2 *(6.8±0.7)*	23±1
MC-Cellulose	25±5 *(54±7)*	7±2 *(19±9)*	/	8±3 *(15±5)*	/	0.6±0.6 *(1±1)*	6±3 *(11±6)*	4.68±0.03
Arabinose	86±7 *(20±3)*	146±46 *(31±8)*	54±6 *(12.5±0.6)*	/	48±17 *(13±5)*	61±30 *(13±5)*	45±3 *(10.5±0.8)*	44±6
Xylose	118±14 *(19±2)*	247±82 *(34±10)*	35±18 *(5±2)*	72±35 *(14±7)*	6±6 *(0.9±0.9)*	104±16 *(18±4)*	62±11 *(9.6±0.7)*	64.4±0.9
Xylan	111±20 *(35±7)*	88±50 *(26±14)*	8±2 *(2.4±0.4)*	12±7 *(4±2)*	/	83±19 *(25±6)*	21±3 *(7±1)*	32±2
Wheat Straw	38±7 *(50±5)*	26±3 *(35±5)*	4±2 *(5±2)*	4.7±0.6 *(6.3±0.8)*	/	0.7±0.7 *(1±1)*	1.6±0.7 *(2±1)*	8±1

Table

Table 3: Hydrogen yields, metabolic patterns and main identified bacteria obtained from dark fermentation performed on different inocula and substrates in the literature. Units of hydrogen yield, H_2 column, correspond to a) $mol_{H2}.mol^{-1}_{substrate}$, b) $mmol_{H2}.g^{-1}_{VS}$, c) $mmol_{H2}.g^{-1}_{substrate}$, d) $mmol_{H2}.g^{-1}_{TVS}$ and e) $mmol_{H2}./g^{-1}_{DCO}$. Metabolites are expressed in % of COD converted and abbreviations correspond to Acetate (HAc), Butyrate (HBut); Caproate (HCap), Ethanol (EtOH), Lactate (HLac), Propionate (Hpr), Formate (Hfor), Valerate (HVal) and Succinate (HSuc).

Inoculum	Substrate	H2	HAc	HBut	EtOH	HPr	HLac	HFor	HVal	HCap	HSuc	HiBut	Major Bacteria	References
anaerobically-digested sludge	fructose	1.84 [a]	34%	59%	6%	/	1%	/	/	0%	/	/	C. sporogenes	(Quéméneur et al., 2011)
	glucose	1.79 [a]	33%	60%	6%	/	1%	/	/	0%	/	/	C. sporogenes	
	sucrose	1.67 [a]	86%	13%	1%	/	0%	/	/	0%	/	/	C. sporogenes	
	maltose	1.65 [a]	36%	58%	4%	/	0%	/	/	1%	/	/	C. acetobutylicum	
	cellobiose	1.56 [a]	35%	52%	9%	/	2%	/	/	1%	/	/	C. cellulolyicum; C. sporogenes; C. Saccharobutylicum ; C. kluyveri; C. acetobutylicum	
	maltotriose	1.38 [a]	31%	48%	17%	/	3%	/	/	1%	/	/	C. acetobutylicum	
hot spring culture	xylose	0.7 [a]	25%	34%	5%	0%	1%	34%	/	/	/	/	C. acetobutylicum; C. tyrobutyricum	(Mäkinen et al., 2012)
	arabinose	0.42 [a]	23%	31%	13%	0%	8%	25%	/	/	/	/	/	
seed sludge	xylose	2.24 [a]	17%	62%	13%	8%	/	/	/	/	/	/	C. saccharobutylicum; Clostridiales sp	(Qiu et al., 2016)
anaerobic activated sludge	rice straw	6 [d]	67%	25%	7%	/	/	/	/	/	/	/	Clostridium sp.	(Cheng et al., 2011)
C. butyricum AS1.209	Corn straw	2.6 [c]	46%	28%	7%	19%	/	/	/	/	/	/	C. butyricum AS1.209 (%)	(Li and Chen, 2007)
Mesophilic digested sludge	Starch	6.1 [e]	15%	80%	2%	0%	0%	3%	/	/	0%	/	C. acetobutylicum; C. butyricum	(Akutsu et al., 2009)
Soybean meal		5.6 [e]	27%	40%	31%	0%	0%	2%	/	/	0%	/	C. acetobutylicum; C. butyricum	
Kitchen Waste		5.1 [e]	20%	71%	2%	0%	0%	6%	/	/	1%	/	C. paraputrificum; Citrobacter freufii	
Cattle Manure		4.6 [e]	23%	49%	22%	0%	0%	7%	/	/	0%	/	C. acetobutylicum; C. butyricum	
Activated Sludge		3.5 [e]	36%	5%	54%	2%	0%	3%	/	/	0%	/	Bacteroides eggerthii; C.	

Inoculum	Substrate	H2	HAc	HBut	EtOH	HPr	HLac	HFor	HVal	HCap	HSuc	HiBut	Major Bacteria	References
													pasteurianum	
Thermophilic Digested Sludge		2.2 [e]	42%	7%	51%	0%	0%	0%	/	/	0%	/	Clostridium sp.; Bacillus sp.	
Soil		2 [e]	31%	2%	51%	10%	0%	2%	/	/	4%	/	Bacteroides eggerthii	
Thermophilic Acidogenic Sludge		0.7 [e]	22%	0%	66%	0%	1%	4%	/	/	7%	/	Bacteroides sp.; C. aminovalericum	
Manure anaerobic digestate	Glucose	0.60 [a]	2.4%	14%	5.5%	/	76%	/	/	/	/	/	*Clostridium* sp.; *Bacillus* sp. *Paenibacillus* sp.	*This study*
	Cellobiose	0.36 [a]	5%	5%	11%	/	73%	/	/	/	/	/	*Bacillus* sp. *Paenibacillus* sp.	
	MCC	6 [e]	54%	19%	1%	8%	/	/	/	/	/	/	*Ruminococcaceae*	
	Arabinose	0.45 [a]	20%	31%	13%	/	13%	/	/	/	/	12.5%	*Clostridium* sp.; *Bacillus* sp. *Paenibacillus* sp.	
	Xylose	0.62 [a]	19%	34%	18%	14%	0.9%	/	/	/	/	5%	*Clostridium* sp.; *Bacillus* sp. *Paenibacillus* sp.	
	Xylan	21 [e]	35%	26%	25%	4%	/	/	/	/	/	2.4%	*Ruminococcaceae;* *Clostridium* sp.; *Bacillus* sp. *Paenibacillus* sp.	
	Wheat straw	1.6 [e]	50%	35%	1%	6.3%	/	/	/	/	/	5%	*Ruminococcaceae*	